Physical and electrochemical properties of supercapacitor composite electrodes prepared from biomass carbon and carbon from green petroleum coke

Awitdrus, M. Deraman, I. A. Talib, R. Farma, R. Omar, M. M. Ishak, E. Taer, B. N. M. Dolah, N. H. Basri, and N. S. M. Nor

Citation: AIP Conference Proceedings **1656**, 030007 (2015); doi: 10.1063/1.4917096
View online: http://dx.doi.org/10.1063/1.4917096
View Table of Contents: http://scitation.aip.org/content/aip/proceeding/aipcp/1656?ver=pdfcov
Published by the AIP Publishing

Articles you may be interested in

Effect of carbonization temperature on the physical and electrochemical properties of supercapacitor electrode from fibers of oil palm empty fruit bunches
AIP Conf. Proc. **1656**, 030005 (2015); 10.1063/1.4917094

Binderless Composite Electrode Monolith from Carbon Nanotube and Biomass Carbon Activated by KOH and CO 2 Gas for Supercapacitor
AIP Conf. Proc. **1415**, 180 (2011); 10.1063/1.3667251

Binderless Composite Electrode Monolith from Carbon Nanotube and Biomass Carbon Activated by H 2 SO 4 and CO 2 Gas for Supercapacitor
AIP Conf. Proc. **1415**, 175 (2011); 10.1063/1.3667250

Electrical Conductivity Of Carbon Pellets Prepared From Mixtures Of Pyropolymers From Oil Palm Bunches and Petroleum Green Coke
AIP Conf. Proc. **1325**, 50 (2010); 10.1063/1.4757187

Electrochemical properties of carbon nanofiber web as an electrode for supercapacitor prepared by electrospinning
Appl. Phys. Lett. **83**, 1216 (2003); 10.1063/1.1599963

Repository University Of Riau
PERPUSTAKAAN UNIVERSITAS RIAU
http://repository.unri.ac.id/

This article is copyrighted as indicated in the article. Reuse of AIP content is subject to the terms at: http://scitation.aip.org/termsconditions. Downloaded to IP: 103.10.169.198 On: Mon, 20 Apr 2015 03:49:38

Physical and Electrochemical Properties of Supercapacitor Composite Electrodes Prepared from Biomass Carbon and Carbon from Green Petroleum Coke

Awitdrus[1, 2], M. Deraman[1, *], I. A. Talib[1], R. Farma[1, 2], R. Omar[1], M. M. Ishak[1], E. Taer[1, 2], B. N. M. Dolah[1], N. H. Basri[1] and N. S. M. Nor[1]

[1]*School of Applied Physics, Faculty of Science and Technology, Universiti Kebangsaan Malaysia, 43600 Bangi, Selangor, Malaysia*
[2]*Department of Physics, Faculty of Mathematics and Natural Sciences, University of Riau, 28293 Pekanbaru, Riau, Indonesia*
**Email: madra@ukm.my*

Abstract. The green monoliths (GMs) were prepared from the mixtures of pre-carbonized fibers of oil palm empty fruit bunches (or self-adhesive carbon grains (SACG)) and green petroleum coke (GPC) with the mixing ratio of 0, 10, 30, 50 and 70 % GPC, respectively. The GMs were carbonized in N_2 environment at 800°C to produce carbon monoliths (CM00, CM10, CM30, CM50 and CM70). The CMs were CO_2 activated at 800°C for 1 hour to produced activated carbon monolith electrodes (ACM00, ACM10, ACM30, ACM50 and ACM70). For each percentage of GPC, three duplicate symmetrical supercapacitor cells were fabricated using these activated carbon monolith electrodes respectively, and the capacitive performance amongst the cells was compared and analyzed in order to observe the relationship between the capacitive performance and the physical properties (microstructure and porosity) of the ACMs electrodes containing varying percentage of GPC.

Keywords: *Activated carbon monoliths, Supercapacitor, Electrochemical properties, Porosity, Microstructure.*
PACS: 81.05.U-, 82.47.Uv, 84.37.+q, 68.43.-h, 81.40.-z

INTRODUCTION

Supercapacitor is the energy storage device that has a high capacitance value, rapidly charge-discharge processes and long life cycle. Electrode, electrolyte, current collector and the separator are the main components of supercapacitor. Energy storage occurs when the ionic charge of the electrolyte and the electronic charge of the electrode form a double layer on the surface of meso- and micro-pores. As the distance between a double layer is very small (a few nm) depending on the type of electrolyte, and the pore surface area is very large (~ 500 to 1500 m^2g^{-1}) then supercapacitor will have a high capacitance value (~ unit Farad). In Ragone plot, the range of specific energy and specific power of supercapacitor is between conventional capacitors and batteries [1]. Supercapacitor is widely used in industry, information technology, electronic devices, hybrid electric vehicles, military equipment, digital communication systems, digital cameras, power supply without interruption and pulsed laser techniques [2,3].

Carbon is suitable for supercapacitor electrodes application because it possesses a unique combination of physical and chemical properties, i.e. (i) high electrical conductivity, (ii) high surface area, (iii) good corrosion resistance, (iv) high temperature stability, (v) pore structure which can be controlled, (vi) can be processed and is compatible with other components in composite materials [1]. Carbon can be produced from organic materials such as hydrocarbon gas, petroleum, coal, polymers and biomass. List of biomass materials that have been used as supercapacitor electrodes, i.e. coffee, seaweed, sugarcane bagasse, wheat stems, corn, coconut husks and walnut shell can be found in Taer et al. [4]. In addition, green petroleum coke has also been used as a precursor for supercapacitor electrodes [5-7].

In the present study, the material used to produce carbon electrode supercapacitor is a self-adhesive carbon grain (SACG) [8] from fiber of oil palm empty fruit bunches (EFB) and green petroleum coke (GPC). Percentage of GPC in SACG and GPC mixtures were varied from 0 to 70 percent in order to determine the GPC effect on the physical and electrochemical properties of electrodes. The main difference between SACG and GPC is that SACG has 42-43% carbon content and has an adhesive property [8] while GPC contains 80-90% carbon and is non-adhesive.

Repository University Of Riau
PERPUSTAKAAN UNIVERSITAS RIAU
http://repository.unri.ac.id/

Symposium (APS 2012)
030007-5; doi: 10.1063/1.4917096
978-0-7354-1298-9/$30.00

This article is copyrighted as indicated in the article. Reuse of AIP content is subject to the terms at: http://scitation.aip.org/termsconditions. Downloaded to IP: 103.10.169.198 On: Mon, 20 Apr 2015 03:49:38

EXPERIMENTAL

EFB (Sabutek Sdn. Bhd. Malaysia) [9] were pre-carbonized at low temperatures to produce self-adhesive carbon grain (SACG) with grains size ≤ 53 μm using our previous method [10]. GPC (Pertamina UP II Dumai, Indonesia) were also milled to obtain the grains with size ≤ 53 μm. Weight percentages of GPC in the green pellets (GPs) were 0, 10, 30, 50 and 70%. GPs from SACG and GPC were prepared in a mould with a diameter of 20 mm and a compression pressure of 7.5 metric tones and then carbonized at a temperature of 800°C in N_2 environment (1.5 l/min) using multi step heating profile to produce carbon monoliths (CMs) [11]. CMs were then activated at a 800°C for 1 hour with CO_2 flow rate of 1 liter per minutes. ACMS were identified as the ACM00, ACM10, ACM30, ACM50 and ACM70 that is corresponding to 0, 10, 30, 50 and 70% by weight percentage of GPC, respectively.

Microstructure characterization of ACMs was done using FESEM (Supra PV 55 model). Parameters of porosity (BET surface area, micro pore area, total pore volume and average pore diameter) were determined from N_2 adsorption-desorption isotherm data at 77 K experiment using accelerated surface area and porosimeter system (Micromeretics ASAP 2010).

Supercapacitor cells were fabricated using the ACMs, current collector (Stainless steel 316L), sulfuric acid (1 M) as electrolyte solution and teflon (0.2 mm) as the separator. Characterization of supercapacitor performance using electrochemical impedance spectroscopy (EIS), cyclic voltammetry (CV) and galvanostatic charge and discharge (GCD) methods was conducted by using Solartron 1286 and Solartron 1255HF electrochemical interface frequency response analyzer. Specific capacitance of supercapacitor cells was calculated based on the characterization method used, the EIS, CV and GCD, respectively, using the respective equations (1), (2) and (3) [2]

$$C_{sp} = -\frac{1}{\pi f Z'' m} \quad (1)$$

$$C_{sp} = \frac{2i}{S m} \quad (2)$$

$$C_{sp} = \frac{2i}{\Delta V/_{\Delta t} m} \quad (3)$$

where m is the weight of electrode, f is the frequency (Hz), Z" is the imaginary part of impedance (Ω), i is the electric current (A), S is the scan rate (mV / s), ΔV is the voltage (V) and Δt is the time (s), ΔV and Δt are taken from the discharge curve of the GCD data. The specific energy and specific power were calculated from discharge curve of the GCD data using equations (4) and (5), respectively.

$$E = \frac{Vit}{m} \quad (4)$$

$$P = \frac{Vi}{m} \quad (5)$$

RESULTS AND DISCUSSION

FESEM micrograph analysis of the fracture surface of ACMs with magnification of 5 kX showed that all electrodes are highly porous, and there is an open large macropores (~in units of microns) between grains with different size and randomly distribution throughout the sample. For all electrodes, fractured surface of grains are smoother than the surface of the grain boundary fracture. Fracture at the grain boundary are more prevalent in the electrodes with lower GPC content; it can be interpreted as the addition of GPC contributed to increase bonding forces between grains boundary. Smaller macro pores on the surface and inside the grains are not visible in the micrograph at this magnification and so with the magnification of 50 kX. To illustrate these properties, Figure 1 shows the micrographs of electrode with 0% GPC and 70% GPC at magnification of 5 kX.

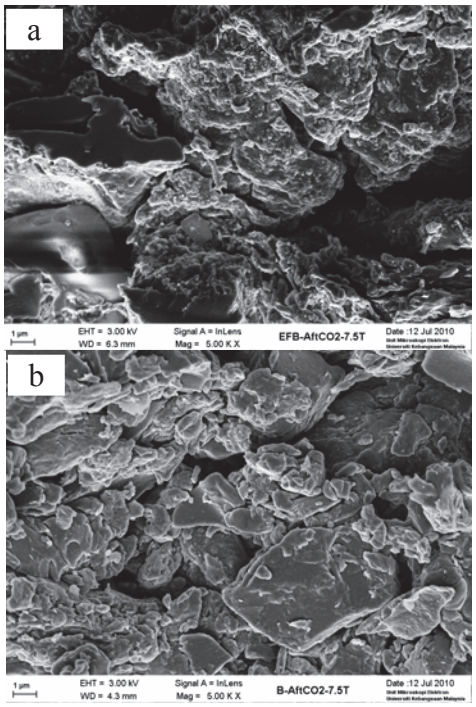

FIGURE 1. FESEM micrographs of (a) ACM00, (b) ACM70.

Repository University Of Riau
PERPUSTAKAAN UNIVERSITAS RIAU
http://repository.unri.ac.id/

This article is copyrighted as indicated in the article. Reuse of AIP content is subject to the terms at: http://scitation.aip.org/termsconditions. Downloaded to IP: 103.10.169.198 On: Mon, 20 Apr 2015 03:49:38

Data of N_2 adsorption-desorption isotherms at 77 K for all ACMs in Figure 2 shows that all electrodes are micro-porous materials (type I isotherm [12]) and the addition of GPC reduced adsorption-desorption capacity. BET surface area (S_{BET}), micro area (S_{Micro}), meso area (S_{Meso}), micro volume (V_{Micro}) and meso (V_{Meso}) and the pore diameter (D) calculated from Figure 2 are shown in Table 1. The results in the table show that the addition of GPC reduced micropores and mesopores in the electrodes. The trend of such a reduction in pores also occurs in the electrodes that contain a mixture of activated carbon and carbon nanotube [13], and a mixture of activated carbon and clay [14], and a mixture of activated carbon and carbon nanotube, and activated carbon and graphite [15].

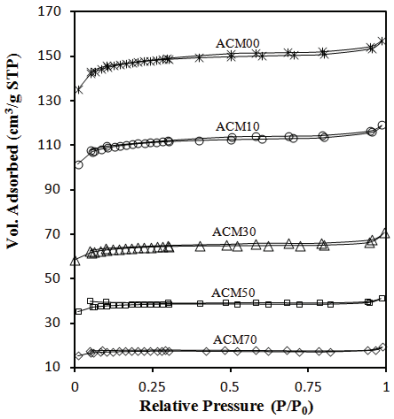

FIGURE 2. Nitrogen adsorption-desorption isotherm data of ACMs at 77K.

S_{BET} obtained in the present study is smaller than the S_{BET} reported for activated carbon from a mixture of activated carbon from SACG and carbon nanotube (485 m^2/g) [12], S_{BET} = 61-766 m^2/g for a mixture of activated carbon and clay [13], and S_{BET} = 540.4 m^2/g for a mixture of activated carbon and nano-TiO_2 [15]. Micropores and mesopores formed in electrodes supercapacitor can affect the movement of electrolyte ions and play an important role to the value of specific energy and specific power [16]. Chemical activation of GPC was found to produce better results [6,7] compared to physical activation used in this study.

TABLE 1. Porosity parameters of the ACMs

Samples	ACM 00	ACM 10	ACM 30	ACM 50	ACM 70
S_{BET} (m^2/g)	447.6	335.8	193.8	116.5	52.9
S_{Micro} (m^2/g)	398.9	298.4	173.4	104.8	47.5
S_{Meso} (m^2/g)	48.6	37.4	20.4	11.6	5.4
V_{Micro} (cm^3/g)	0.207	0.155	0.090	0.054	0.025
V_{Meso} (cm^3/g)	0.037	0.030	0.020	0.010	0.005
Diameter (Å)	30.70	32.34	39.10	33.58	46.96

The EIS data (Nyquist plot) in the range of frequencies 10^6 - 0.1 Hz for ACMs cells are shown in Figure 3. Semicircle in high frequency region (~ 79432<f<398 Hz) represents the dominant resistive nature of the system electrode/electrolyte/collector-current. Straight line with slope 45° (Waburg diffusion) in the middle frequency region (~2511<f<4 Hz) represents the combination of resistive behavior from the resistance of ions penetrating into the pores and capacitive behavior due to an increase of more ions penetrating the pores. Straight lines at the low frequency region (~31<f<0.1 Hz) represents the dominant of capacitive behavior from formation of ionic charge and electronic charge of double layer systems at the surface of micro pores because at this frequency the ions more easily diffuse into the micropores [17 -20]. For all the frequencies region, the Nyquist plot looks different for the electrode with different weight percentage of GPC, this indicates the presence of GPC can change the electrochemical properties of the electrode. The maximum specific capacitance calculated by using equation (1) at low frequency (0.1 Hz), as shown in Table 2, are found to decrease with increasing weight percentage of GPC.

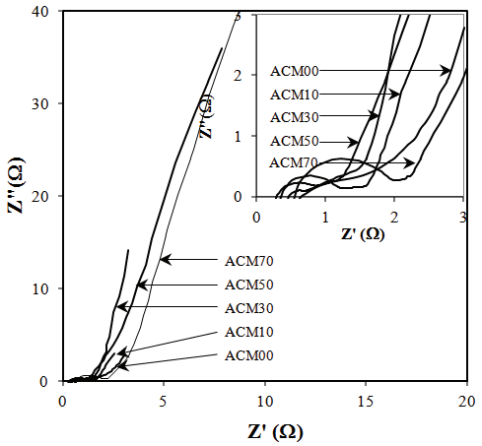

FIGURE 3. Nyquist plot of the ACMs cells.

TABLE 2. Average specific capacitance taken from three duplicated measurements of the ACMs cell using EIS, CV and GCD methods

Cells	Specific capacitance (F/g)		
	EIS	CV	GCD
ACM00s	15.453	23.024	20.191
ACM10s	12.438	17.556	14.137
ACM30s	2.473	8.472	4.559
ACM50s	0.999	1.866	1.725
ACM70s	0.630	2.780	0.759

Cyclic voltammograms for ACMs supercapacitor cell are shown in Figure 4 with potential range -1 - 1 V and scan rate 5 mV/s. Data for the ACM00 cell has no redox peaks and the data profile like a rectangular like

Repository University Of Riau
PERPUSTAKAAN UNIVERSITAS RIAU
http://repository.unri.ac.id/

This article is copyrighted as indicated in the article. Reuse of AIP content is subject to the terms at: http://scitation.aip.org/termsconditions. Downloaded to IP: 103.10.169.198 On: Mon, 20 Apr 2015 03:49:38

shape indicates that the charge-discharge is based on electrostatic process. Data for cells ACM10 - ACM70 have a redox peak in the middle of potential region (~ 0 V); that means the charge-discharge reactions occur based on faradaic or in other words, these cells are pseudocapacitors. The maximum redox peak is found in the cell ACM30. The specific capacitances calculated from the data in Figure 4 using equation (2) are shown in Table 2.

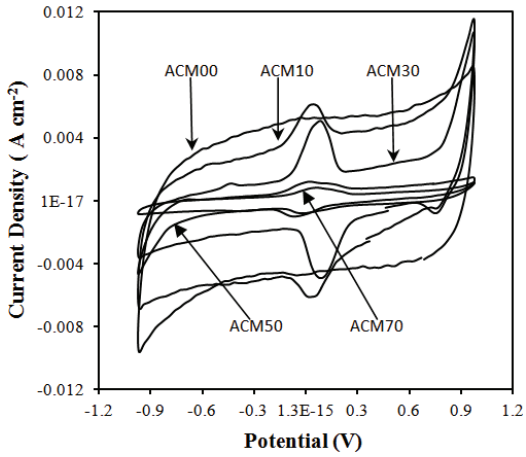

FIGURE 4. Cyclic voltammogram of ACMs cells.

Cycle voltammograms at scan rates of 5, 15, 25, 50 and 100 mV/s for all the cells were used to calculate the specific capacitance and the results are shown in Figure 5. For larger scan rates, cycle times are shorter, then the electrolyte ions do not have enough time to diffuse into pores but if the scan rate is lower, the ions will have enough time to diffuse into pores because the cycle period is longer [21]. Thus, as shown by the results in Figure 5, the specific capacitance value is decreased with increasing scan rate. It is apparent that as the weight percentage of GPC increases, the C_{sp} becomes less dependence on the scan rate. The decrease in specific capacitance with increasing scan rate is due to the limited transfer of ions to the surface of carbon particle, resulting in inaccessible pore portions of the electrode layer at this scan rate. This phenomenon is typical for all types of supercapacitors, reflecting the limited mass transfer kinetics within the porous electrode [22].

GCD curves for all ACMs cells at constant current density of 7 mA/cm^2 and the potential range of 0-1 V are shown in Figure 6. It can be seen that increasing the weight percent of GPC shortens the time interval of charge discharge process; that means the current capacity is smaller [23]. The specific capacitance, calculated from the data in Figure 6 using equation (3), shown in Table 2, seems to decrease with increasing GPC in the electrode.

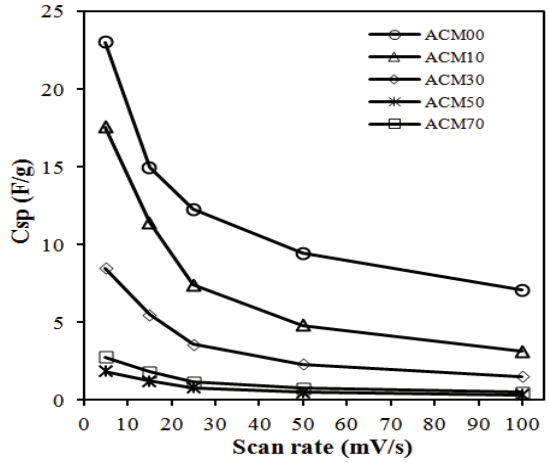

FIGURE 5. Specific capacitance of ACMs cells with different scan rate.

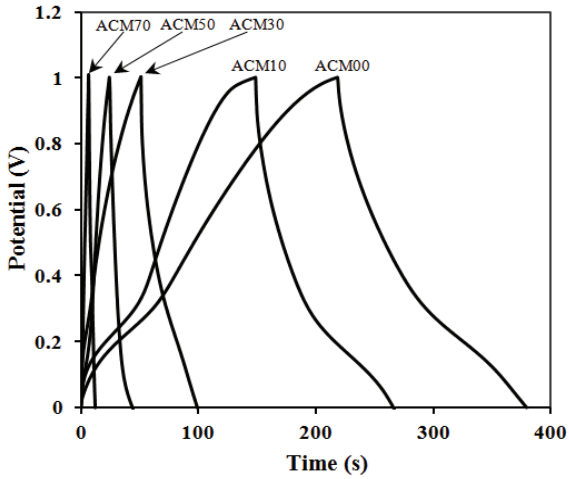

FIGURE 6. Galvanostatic charge-discharge of the ACMs cells with current of 7 mA/cm^2.

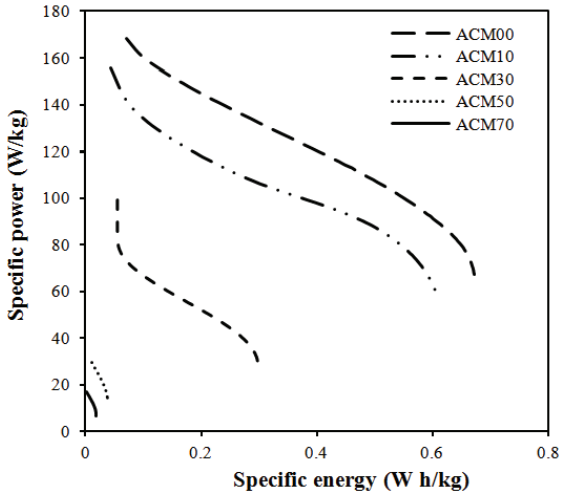

FIGURE 7. Specific energy and specific power of the ACMs cells.

Repository University Of Riau
PERPUSTAKAAN UNIVERSITAS RIAU
http://repository.unri.ac.id/

This article is copyrighted as indicated in the article. Reuse of AIP content is subject to the terms at: http://scitation.aip.org/termsconditions. Downloaded to IP: 103.10.169.198 On: Mon, 20 Apr 2015 03:49:38

Specific energy and specific power of ACMs cells calculated using equations (4) and (5) are shown in the form of Ragone plot in Figure 6. The plots clearly show that (i) the specific power decreases with increasing specific energy, where the slope of decline is more pronounced when the weight percentage of GPC is higher, and (ii) the magnitude of specific energy and specific power decreases significantly when the weight percentage of GPC is higher.

CONCLUSIONS

Supercapacitor electrodes were prepared by carbonization of the mixtures containing pre-carbonized EFB and varying percentage of GPC (0 to 70%). The increase of GPC percentage in electrodes was found to change the physical property of electrodes (significant reduction in micropores volume) and hence did not improve the capacitive performance of the supercapacitor cells (significant reduction in specific capacitance, specific power and specific energy). These results are associated with the effect that during the activation, carbon from GPC did not promote the formation of more quntities of pore (micro and meso) in the electrode; the higher the GPC percentage corresponds to the more severe effect.

ACKNOWLEDGMENTS

The authors acknowledge the Research University Grant (UKM-GUP-2011-216, UKM-DLP-2012-022 and UKM-DLP-2012-023), Centre for Research and Innovation Management (CRIM) UKM and the assistance of Mr. Saini Sain.

REFERENCES

1. A. G. Pandolfo and A. F. Hollenkamp, *J. Power Sources* **157**, 11-27 (2006).
2. C. Portet, P. L. Taberna, P. Simon, E. Flahaut and C. Laberty-Robert, *Electrochim. Acta* **50**, 4174-4181 (2005).
3. Y. Zhang, H. Feng, X. B. Wu, L. Z. Wang, A. Q. Zhang, T. C. Xia, H. C. Dong, X. F. Li and L. S. Zhang, *Int. J. Hydrogen Energy* **34**, 4889-4899 (2009).
4. E. Taer, M. Deraman, I. A. Talib, Awitdrus, S. A. Hashmi and A. A. Umar, *Int. J. Electrochem. Sci* **6**, 3301-3315 (2011).
5. V. Ruiz, C. Blanco, R. Santamaria, J. M. Ramos-Fernandez, M. Martinez-Escandell, A. Sepulveda-Escribano and F. Rodriguez-Reinoso, *Carbon* **47**, 195-200 (2009).
6. G. W. Sun, D. H. Long, X. J. Liu, W. M. Qiao, L. Zhan, X. Y. Liang and L. C. Ling, *J. Electroanal. Chem* **659**, 161-167 (2011).
7. M. X. Wang, C. Y. Wang, M. M. Chen, Y. S. Wang, Z. Q. Shi, X. Du, T. Q. Li and Z. J. Hu, *New Carbon Mater* **25**(4), 285-290 (2010).
8. M. Deraman, R. Omar and A. G. Harun, *J. Mater. Sci. Lett.* **17**, 2059-2060 (1998).
9. M. Deraman, S. Zakaria and J. A. Murshidi, *Jpn. J. Appl. Phys* **40**(5A), 3311-3314 (2001).
10. M. Deraman, S. Zakaria, R. Omar and A. A. Aziz, *Jpn. J. Appl. Phys* **39**, L1236-L1238 (2000).
11. M. Deraman, R. Omar, S. Zakaria, I. R. Mustapa, M. Talib and N. Alias, *J. Mater. Sci* **37**, 3329-3335 (2002).
12. M. Khalfaoui, S. Knani and M. A. Hachicha, A. Ben Lamine, *J. Colloid Interface Sci* **263**, 350-356 (2003).
13. R. Farma, M. Deraman, R. Omar, Awitdrus, M. M. Ishak, E. Taer and I. A. Talib, "Binderless Composite Electrode Monolith from Carbon Nanotube and Biomass Carbon Activated by H2SO4 and CO2 Gas for Supercapacitor" in *The 4th Nanoscience and Nanotechnology Symphosium (NNS)-2011,* edited by F. Iskandar et al., AIP Conference Proceedings 1415, American Institute of Physics, Melville, NY, 2011, pp 180-184.
14. M. Yates, M. A. Martin-Luengo, L. V. Argomaniz and S. N. Velasco, *Micropor. Mesopor. Mater* **154**, 87-92 (2012).
15. Y. Huai, X. Hu, Z. Lin and J. Suo, *Mater. Chem. Phys* **113**, 962-966 (2009).
16. T. E. Rufford, D. Hulicova-Jurcakova, K. Khosla, Z. Zhu and G.Q. Lu, *J. Power Sources* **195**, 912-918 (2010).
17. W. -C. Chen, T. -C. Wen and H. Teng, *Electrochim. Acta* **48**, 641-649 (2003).
18. F. Rafik, H. Guolous, R. Gallay, A. Crausaz and A. Berthon, *J. Power Source* **165**, 928-934 (2007).
19. Y. -R. Nian and H. Teng, *J. Electroanal. Chem* **540**, 119-127 (2003).
20. J. Gamby, P. L. Taberna, P. Simon, J. F. Fauvarque and M. Chesneau, *J. Power Sources* **101**, 109-116 (2001).
21. Awitdrus, M. Deraman, I. A. Talib, R. Farma, R. Omar, M. M. Ishak, N. H. Basri and B. N. M. Dolah, *Advanced Material Research* **501**, 13-18 (2012).
22. K. C. Tsay, L. Zhang and J. Zhang, *Electrochim. Acta* **60**, 428-436 (2012).
23. C. Kim, *J. Power Sources* **142**, 382-388 (2005).

Repository University Of Riau
PERPUSTAKAAN UNIVERSITAS RIAU
http://repository.unri.ac.id/

This article is copyrighted as indicated in the article. Reuse of AIP content is subject to the terms at: http://scitation.aip.org/termsconditions. Downloaded to IP: 103.10.169.198 On: Mon, 20 Apr 2015 03:49:38